Volume 1 | Number 1 | Jan 2013 | Pages 1–100

Dalton Transactions

An international journal of inorganic chemistry
www.rsc.org/dalton

ROYAL SOCIETY OF CHEMISTRY

This is an *Accepted Manuscript*, which has been through the Royal Society of Chemistry peer review process and has been accepted for publication.

Accepted Manuscripts are published online shortly after acceptance, before technical editing, formatting and proof reading. Using this free service, authors can make their results available to the community, in citable form, before we publish the edited article. We will replace this *Accepted Manuscript* with the edited and formatted *Advance Article* as soon as it is available.

You can find more information about *Accepted Manuscripts* in the **Information for Authors**.

Please note that technical editing may introduce minor changes to the text and/or graphics, which may alter content. The journal's standard **Terms & Conditions** and the **Ethical guidelines** still apply. In no event shall the Royal Society of Chemistry be held responsible for any errors or omissions in this *Accepted Manuscript* or any consequences arising from the use of any information it contains.

www.rsc.org/dalton

Dalton Transactions

Dynamic Article Links ▶

ARTICLE TYPE

Self-assembled nanostructures of amphiphilic Zinc(II) salophen complexes: role of the solvent on their structure and morphology†

Ivan Pietro Oliveri, Graziella Malandrino* and Santo Di Bella*

5 *Dipartimento di Scienze Chimiche, Università di Catania, I-95125 Catania, Italy.*
*E-mails: gmalandrino@unict.it (G.M.), sdibella@unict.it (S.D.B).
†*Electronic supplementary information (ESI) available: Additional FE-SEM and XRD data. See DOI: 10.1039/b000000x*

10 This contribution explores the effect of some solvent properties, such as volatility, polarity, and Lewis basicity on the formation of molecular self-assembled nanostructures in the solid state, obtained either by casting from related solutions or by complete solvent evaporation, using seven solvents representative of common classes of coordinating organic solvents, of an amphiphilic Zn^{II} Schiff-base complex. In all cases, the existence of defined X-ray diffraction patterns, both in cast and powder samples, indicates the strong tendency towards the 15 molecular self-assembly of such complexes. While nanostructures from acetone, THF, pyridine, and DMF have a lamellar organization, those from ACN, ethanol, and DMSO exhibit a 2D columnar square structure. Field emission scanning electron microscopy analysis indicates that nanostructures from volatile acetone, THF, ACN, and ethanol solvents show a fibrous morphology, while those from the low volatile pyridine, DMF, and DMSO reveal a ribbon appearance. Overall, results indicate that while the formation of such nanostructures is 20 independent from the Lewis basicity of the solvent, the solvent polarity affects their structure - more polar solvents favour higher symmetry structures, and the solvent volatility influences their morphology and the order in the cast films - lower volatility of the solvent parallels the formation of much more ordered structures. Therefore, the appropriate choice of the solvent allows controlling the structure, morphology, and order of these molecular assemblies.

Introduction

25 The molecular self-assembly and control of the supramolecular architecture is a widely explored field of research, involving both fundamental[1-3] and application aspects,[4] and represents a challenge of the modern supramolecular chemistry. This process 30 is generally driven by noncovalent weak interactions, such as π-π stacking, hydrogen bonding, electrostatic, and van der Waals forces.[1-3]

A very different approach for the formation of supramolecular species is offered by transition-metal complexes in which 35 molecular aggregation is driven through metal-ligand coordination.[5] For example, the molecular aggregation via intermolecular Zn···O interactions in some Zn^{II} Schiff-base complexes provided new possibilities to tailor their supramolecular architecture, both in the solid state and in 40 solution.[6,7] Actually, bis(salicylaldiminato)Zn^{II} complexes are Lewis acidic species,[8] which saturate their coordination sphere by coordinating a variety of Lewis bases[8-10] or, in their absence, can be stabilized through intermolecular Zn···O axial coordination involving the phenolic oxygen atoms of the ligand framework.[11] 45 We have recently demonstrated that a series of amphiphilic Zn(salophen) Schiff-base complexes, having alkoxy substituents

as lateral groups in the salicylidene rings, self-assemble into nanofibers.[12] In particular, fibrous aggregates are always obtained from solutions of coordinating solvents, either by drop casting or 50 by complete solvent evaporation, while in the case of noncoordinating solvents, where oligomeric aggregates are already present in solution, no formation of nanofibers is observed. The morphology of nanofibers is independent from the used method, drop casting or solvent evaporation, and from alkyl 55 side chains length of complexes. Moreover, the length of side alkyl groups and their degree of interdigitation influence the average spacing, as derived by XRD analysis. Although in solution of coordinating solvents these complexes are present as monomeric adducts having the solvent axially coordinated, 60 nanofibers are mainly stabilized through intermolecular Zn···O interactions upon solvent evaporation. Thus, the removal of the coordinated solvent leaves a vacant coordination site around the Zn^{II} metal centre that is then saturated by intermolecular Zn···O interactions.[12]

65 In this context, it is of interest to further explore the role of the involved solvent to control and shed light on the molecular self-assembly of these complexes, for the design of new molecular structures and materials.[13] In this paper we report a detailed investigation, by means of a combined, field emission scanning

electron microscopy/X-ray diffraction (FE-SEM/XRD) study, on the aggregation properties of these Zn(salophen) complexes using seven solvents, representative of common classes of coordinating organic solvents, with different volatility, polarity, and Lewis

5 basicity. It represents a systematic study, for the first time in any detail, about the solvent effects on the structure and morphology of molecular assembled nanostructures of a transition metal complex in solid state. Actually, literature studies of solvent effects on molecular nanostructures are related to gels[14] or two-

10 dimensional molecular self-assemblies.[15]

It is found that the solvent allows controlling the structure, morphology, and order of these molecular assemblies.

Results

The model compound chosen for the present study is an

15 amphiphilic Zn(salophen) Schiff-base, **1**, having two 4-decyloxy substituents as lateral groups. This allows a sufficient solubility in most common coordinating solvents. On the other hand, longer alkyl groups would not allow enough solubility in polar solvents.
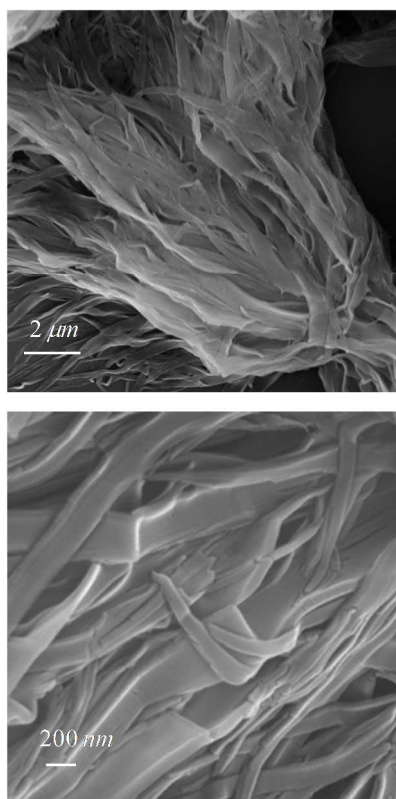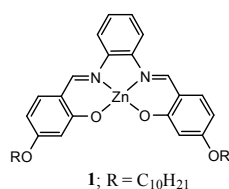
20

1; R = $C_{10}H_{21}$

Fig. 1 FE-SEM images at different magnifications of **1** deposited by casting onto a Si(100) substrate from a DMSO solution.

25 Let us first consider the low volatile, highly polar dimethylsulfoxide (DMSO) solvent and compare the results with those previously obtained with the more volatile, lower polarity tetrahydrofuran (THF) solvent. FE-SEM images of structures obtained by drop-casting from DMSO solutions of **1** onto Si(100)

30 substrates, are shown in Fig. 1. In sharp contrast to our previous results achieved for **1** deposited from solutions of THF,[12] the morphology of resulting structures using DMSO as solvent is very different. Actually, nanoribbons, instead than nanofibers, with width up to ca. 300 nm and length of several microns, are

35 clearly evident in both low and high magnification FE-SEM images.

This different morphology, finds counterpart in XRD patterns, obtained from the cast samples of **1** by X-ray diffraction measurements recorded in grazing incidence mode (Fig. 2). In

40 fact, in comparison to those obtained from THF solutions, XRD patterns are characterized by a sharper signal at 2θ = 3.15°, corresponding to d = 28.05 Å, characteristic of a highly ordered and oriented structure, as also confirmed by the rocking curve measurement of this reflection which indicates a very narrow full

45 width at half maximum, FWHM = 0.035°. Moreover, two low intense signals at 2θ = 4.40° and 7.00°, corresponding to d = 20.08 Å and 12.63 Å, can be identified in the low-angle region of the XRD patterns (Fig. 2). This set of diffraction peaks are with a ratio of almost 1:√2:√5, consistent with a 2D columnar square

50 structure, with a lattice constant of 28.05 Å. Note that, cast films of **1** obtained from THF solutions have a different, less ordered, lamellar structure and do not show any rocking curve.
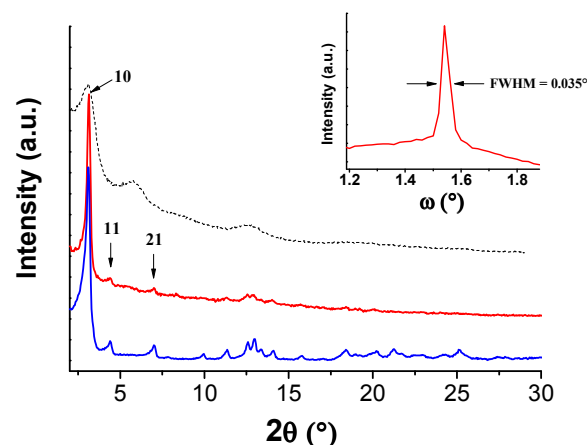

55 **Fig. 2** Comparison of XRD patterns of **1** obtained by casting from a DMSO solution (–), and a dried powder sample obtained from a DMSO solution by complete evaporation of the solvent (–). The dotted line indicates the related XRD pattern of **1** obtained by casting from a THF solution. Inset: rocking curve of the 10 reflection of the cast DMSO

60 sample.

Such nanostructures are observed, from XRD/FE-SEM analysis, even in powder samples of **1** obtained from their DMSO solutions by complete evaporation of the solvent under ambient conditions (Fig. S1†). In such conditions, however, some free

65 DMSO solvent is still present in the powder samples, as results from ^{1}H NMR and UV/vis spectroscopy analysis of the powder sample dissolved in chloroform solution. Then, to remove any residual solvent the powder sample was dried under vacuum,

before further XRD/FE-SEM analyses. The absence of free or chemisorbed solvent, as **1**·DMSO adduct, was further checked by ^{1}H NMR and UV/vis spectroscopy analysis. XRD/FE-SEM analyses of dried powder samples still indicate the existence of defined nanoribbons (Fig. S2†) whose XRD patterns are better defined than those obtained from cast samples (Fig. 2), confirming a 2D columnar square structure.

It is now interesting to explore whether a stronger Lewis base, such as pyridine,[16] affects the aggregation properties of complex **1**. Actually, it is well known that such kind of complexes crystallized from pyridine solutions, or in mixtures of pyridine with other coordinating solvents, always form adducts with pyridine axially coordinated to the Zn[II] metal centre.[17]

XRD patterns of structures obtained either by drop-casting from pyridine solutions of **1** onto Si(100) substrates, or by complete evaporation of the solvent, are shown in Fig. 3. Unexpectedly, defined self-assembled nanostructures are observed even from pyridine solutions, thus indicating that formation of intermolecular Zn····O aggregates leads to more stable structures with respect to the monomeric **1**·pyridine adduct. However, they are quite different, in terms of XRD patterns, than those observed from DMSO solutions, strongly resembling those previously found from THF solutions.[12] In fact, the diffraction patterns of either cast or powder samples show a set of diffraction peaks at 2θ = 3.34°, 6.74°, 10.31°, and 13.72° corresponding to d = 26.45 Å, 13.11 Å, 8.58 Å, and 6.45 Å. The last three peaks can be associated with higher order reflections of the 10 reflection observed at 2θ = 3.34°, thus suggesting a lamellar organization. However, the 10 peak of cast pyridine films, unlike THF cast films, is more intense and sharper and a distinct rocking curve, characteristic of an oriented structure, is observed for this reflection (Fig. 3). The absence of free or chemisorbed solvent, as **1**·pyridine adduct, in the powder pyridine samples was checked by ^{1}H NMR and UV/vis spectroscopy analysis.
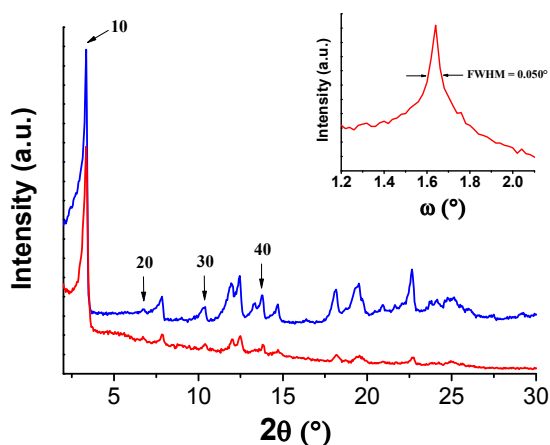

Fig. 3 Comparison of XRD patterns of **1** obtained by casting from a pyridine solution (–), and a powder sample obtained from a pyridine solution by complete evaporation of the solvent (–). Inset: rocking curve of the 10 reflection of the cast sample.

The analysis of FE-SEM images of both cast and powder samples from pyridine solutions offers, however, further surprises (Figs. 4 and S3†). In fact, despite their established lamellar organization, as that previously observed from THF solutions,[12] a

nanoribbon morphology is evident in both cases, as that encountered for nanostructures from DMSO solutions. Moreover, wider nanoribbons, up to 4 µm and several tens of microns long are observed in powder samples.

Finally, cast films and powder samples of **1** obtained from other coordinating solvents of different polarity[18] and volatility, such as acetone, acetonitrile (ACN), ethanol, and dimethylformamide (DMF) were also considered. In particular, XRD patterns of cast films from acetone, ACN and ethanol solutions show low intense, broad peaks resembling those observed from THF solutions, while XRD patterns obtained from DMF solutions are better comparable with those of cast films from pyridine (Fig. 5a). FE-SEM images of both cast and powder samples from acetone, ACN, and ethanol solutions (Figs. 6, S4, S5 and S6†) show a nanofiber morphology, analogously to that previously observed from THF solutions,[12] while FE-SEM images from DMF solutions show a nanoribbon appearance (Figs. S7 and S8†), as that found for nanostructures from pyridine and DMSO solutions.
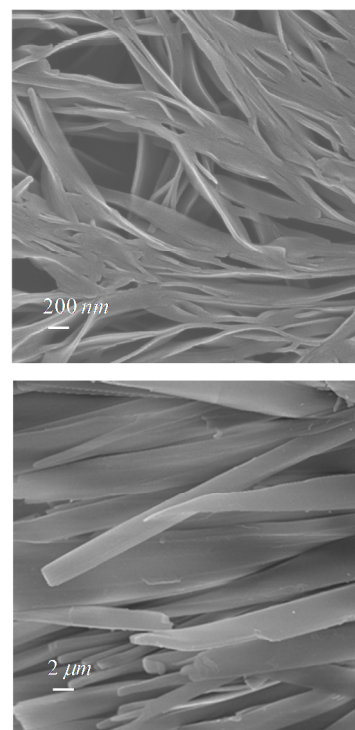

Fig. 4 FE-SEM images of **1** deposited by casting onto a Si(100) substrate from a pyridine solution (top), and a powder sample obtained from a pyridine solution by complete evaporation of the solvent (bottom).

XRD patterns of cast films of all involved solvents are collected in Fig. 5a. Referring to the 10 reflection, it is evident that starting from cast films from acetone, the most volatile solvent, to those obtained from the other progressively less volatile solvents, until DMSO, the lower volatile solvent within the series considered, this reflection initially characterized by a low-intensity, broad peak, becomes progressively sharper and more intense, according with a more ordered nanostructure. Moreover, a rocking curve of the 10 peak can be recorded for films deposited from DMF, as those from pyridine and DMSO, indicative of the formation of nanostructures oriented with respect to the substrate. Analysis of XRD patterns from powder

samples allowed an unambiguous assignment of their structure (Fig. 5b). Thus, a 2D columnar square structure can be established for XRD patterns of powder samples from ACN and ethanol solutions, as found in cast and powder samples from
5 DMSO solutions. Conversely, XRD patterns of powder samples from acetone and DMF solutions are consistent with a lamellar organization, as that observed in powder samples from THF and pyridine solutions. The peaks at higher angles in the XRD patterns observed at the same *2θ* values for all involved solvents
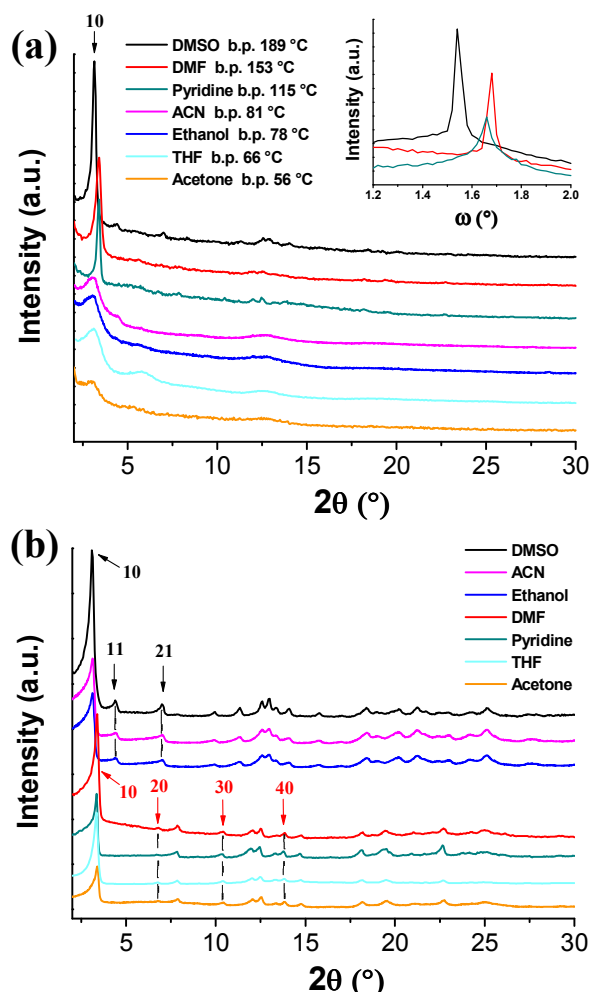10 are probably related to the core molecule.

Fig. 5 (a) XRD patterns of **1** obtained by casting from solutions (c.a. 5.0 × 10⁻⁴ M) of various solvents; (b) powder samples obtained from different solutions by complete evaporation of the solvent.

15 **Table 1** Solvent parameters and nanostructures of **1** from involved solvents

Solvent	Polarity (E_T^N) [a]	Volatility (b.p., °C)	Lewis basicity (DN, kcal/mol) [b]	Structure [c]	Morphology
ethanol	0.654	78	19.2	Col$_{squ}$	nanofibers
ACN	0.460	81	14.1	Col$_{squ}$	nanofibers
DMSO	0.444	189	29.8	Col$_{squ}$	nanoribbons
DMF	0.386	153	30.9	L	nanoribbons
acetone	0.355	56	17.0	L	nanofibers
pyridine	0.302	115	33.1	L	nanoribbons
THF	0.207	66	20.0	L	nanofibers

[a] From ref. 18. [b] Donor number, from ref. 18. [c] Col$_{squ}$= columnar square; L = lamellar.
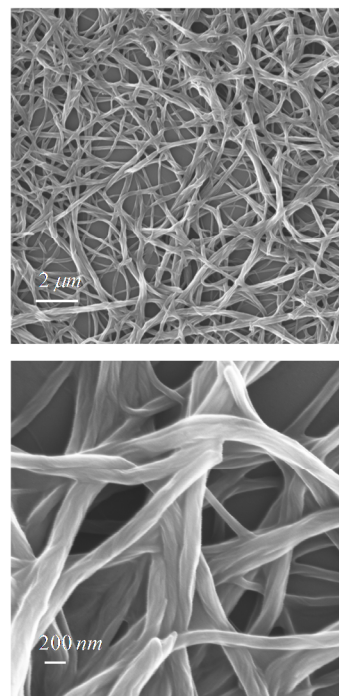

20 **Fig. 6** FE-SEM images at different magnifications of **1** deposited by casting onto a Si(100) substrate from an acetone solution.

Discussion

This work reports a systematic study on the aggregation properties of the amphiphilic Zn(II) Schiff-base complex **1**, in
25 relation to the volatility, Lewis basicity and polarity of the solvent used to prepare the solutions. Nanostructures of **1** obtained from the solutions of involved solvents and related solvent parameters are collected in Table 1. In all considered cases, the existence of defined XRD patterns both in cast and
30 powder samples indicates the strong tendency towards the molecular self-assembly of such complexes, even in different coordinating solvents. Moreover, the analysis of XRD patterns of powder samples unambiguously allowed the assignment of their structure. Thus, while nanostructures from acetone, THF,
35 pyridine, and DMF have a lamellar organization, those from ACN, ethanol, and DMSO exhibit a 2D columnar square structure (Fig. 5). On the other hand, FE/SEM analysis indicates that nanostructures from acetone, THF, ethanol, and ACN show a fibrous morphology, while those from pyridine, DMF, and
40 DMSO reveal a ribbon appearance. Therefore, to rationalize these apparently contrasting results some further comparisons and considerations can be done.

The comparison of present XRD/FE-SEM data from DMSO solutions with those previously obtained from THF solutions
45 allows us to make some other interesting comments and observations. In view of the comparable Lewis basicity of DMSO and THF,[16,18] the different observed behaviour, in terms of structure and morphology, of **1** on passing from THF to DMSO solutions should be related to the much lower volatility (DMSO,
50 b.p. 189 °C *vs*. THF, b.p. 66 °C) and/or stronger polarity of the DMSO solvent.[18] In other words, the solvent evaporation and/or the solvent polarity control the molecular assembly of such species.

To assess whether the polarity is responsible for the different observed structure and/or morphology on passing from THF to DMSO solutions, various solvents of different polarities were considered. In particular, nanostructures from ACN and ethanol solutions exhibit the same, as those from DMSO, 2D columnar square structure. Therefore, given the higher polarity, in terms of E_T^N parameter,[18] of ACN, DMSO, and ethanol ($E_T^N > 0.44$), than that of the other involved solvents (Table 1), we can deduce that the polarity is likely responsible for the different observed structures (lamellar *vs.* 2D columnar square) on passing from THF, pyridine, acetone, and DMF to DMSO, ACN, and ethanol, respectively. That is, the most polar DMSO, ACN, and ethanol solvents favour a higher symmetry structure. Given the amphiphilic nature of **1,** hydrophobic solvent effects should be responsible for the different observed columnar square structure in the case of most polar solvents.

On the other hand, the morphology seems to be influenced by the solvent volatility, independently from its polarity (Table 1). In fact, while nanostructures from the volatile acetone, THF, ethanol, and ACN (boiling points < 80 °C) give nanofibers, those from the low volatile pyridine (b.p. 115 °C), DMF (b.p. 153 °C), and DMSO (b.p. 189 °C) show a nanoribbon morphology.

The solvent volatility also influences the order of the nanostructures in the cast films. Thus, the progressively lower volatility of the solvent, hence slower growing of the molecular aggregates, parallels the formation of much more ordered and oriented structures. This effect seems to be independent from the solvent polarity. In fact, cast films from acetone solutions (the most volatile solvent within the involved series, b.p. 56 °C), despite the larger polarity of acetone with respect to pyridine or THF,[18] lead to the least ordered nanostructures (Fig. 5a).

Finally, formation of these nanostructures seems to be independent from the Lewis basicity of the solvent,[16,18] as they are observed for all involved coordinating Lewis bases solvents. Thus, lamellar structures obtained from pyridine solutions, being pyridine the strongest Lewis base within the series, are also obtained from solutions of acetone having a low Lewis basicity. Analogously, despite the comparable Lewis basicity of ACN and acetone, different, columnar *vs.* lamellar, structures are obtained.

Experimental

Materials

The synthesis of [*N,N*-Bis(4-decyloxy-2-hydroxybenzylidene)-1,2-phenylene-diaminato]Zn[II] (**1**) was previous reported.[8b] All solvents (Aldrich) employed for the present study were used as received.

Measurements

Solution ^{1}H NMR measurements were carried out on Varian Unity Inova 500 MHz spectrometer. Optical absorption spectra were recorded at room temperature with a Varian Cary 500 UV-Vis-NIR spectrophotometer. θ-2θ X-ray diffraction patterns and rocking curves were carried out on a Bruker-AXS D5005 θ-θ X-ray diffractometer, using a Göebel mirror to parallel Cu-K$_\alpha$ radiation, $\lambda = 1.5418$ Å, operating at 40 KV and 30 mA. X-ray patterns were recorded in grazing incidence mode (0.5°) for the cast films and in Bragg-Brentano mode for the powders. Film surface morphology was examined by FE-SEM using a ZEISS SUPRA VP 55 microscope. Samples for XRD measurements were obtained by drop-casting from solutions of complex **1** onto cleaned Si(100) substrates. Samples were subsequently sputtered with gold to avoid charging effects before FE-SEM analysis. Powder samples were obtained by the complete evaporation of the solvent from solutions of complex **1**. FE-SEM analyses were carried out on powders stuck on carbon tape and sputtered with gold.

Conclusions

The control of the molecular assembly into nanoarchitectures is a topic of great, current interest. This contribution explores the effect of some solvent parameters, such as volatility, polarity, and Lewis basicity, on the formation of molecular nanostructures, obtained either by casting from related solutions or by complete solvent evaporation, using seven different coordinating organic solvents, of an amphiphilic Zn[II] Schiff-base complex. Some general trends can be drawn: i) the formation of such nanostructures is independent from the Lewis basicity of the solvent; ii) the solvent polarity affects the structure - more polar solvents favour higher symmetry structures; iii) the solvent volatility affects the morphology - nanofibers are formed from volatile solvents while nanoribbons are formed from low volatile solvents-, and the order of the nanostructures - lower volatility of the solvent parallels the formation of cast films with much more ordered structures. Therefore, the appropriate choice of the solvent allows controlling the structure, morphology, and order of these molecular assembly nanostructures.

Acknowledgment

Notes and references

1. J. W. Steed, D. R. Turner and K. J. Wallace, in *Core Concepts in Supramolecular Chemistry and Nanochemistry*, Wiley; Chichester: U.K., 2007.
2. J.-M. Lehn, in *Supramolecular Chemistry*, VCH: Weinheim, 1995.
3. (*a*) Z. Chen, A. Lohr, C. R. Saha-Möller and F. Würthner, *Chem. Soc. Rev.*, 2009, **38**, 564; (*b*) I. Beletskaya, V. S. Tyurin, A. Yu. Tsivadze, R. Guilard and C. Stern, *Chem. Rev.*, 2009, **109**, 1659; (*c*) F. Würthner, *Chem. Commun.*, 2004, 1564.
4. See, for example: (*a*) Z. Zhao, J. W. Y. Lam and B. Z. Tang, *J. Mater. Chem.*, 2012, **22**, 23726; (*b*) H. -J. Kim, T. Kim and M. Lee, *Acc. Chem. Res.*, 2011, **44**, 72; (*c*) H. Liu, J. Xu, Y. Li and Y. Li, *Acc. Chem. Res.*, 2010, **43**, 1496; (*d*) S. Bhattacharya and S. K. Samanta, *Langmuir*, 2009, **25**, 8378; (*e*) J. A. A. W. Elemans, R. van Hameren, R. J. M. Nolte and A. E. Rowan, *Adv. Mater.*, 2006, **18**, 1251.
5. (*a*) T. R. Cook, Y.-R. Zheng and P. J. Stang, *Chem. Rev.*, 2013, **113**, 734; (*b*) J. K.-H. Hui and M. J. MacLachlan, *Coord. Chem. Rev.*, 2010, **254**, 2363.
6. (*a*) J. K.-H. Hui and M. J. MacLachlan, *Dalton Trans.*, 2010, **39**, 7310; (*b*) J. K.-H. Hui, Z. Yu, T. Mirfakhrai and M. J. MacLachlan, *Chem. Eur. J.*, 2009, **15**, 13456; (*c*) J. K. -H. Hui, Z. Yu and M. J. MacLachlan, *Angew. Chem. Int. Ed.*, 2007, **46**, 7980.
7. See, for example: (*a*) G. Salassa, A. M. Castilla and A. W. Kleij, *Dalton Trans.*, 2011, **40**, 5236; (*b*) S. J. Wezenberg, E. C. Escudero-Adán, J. Benet-Buchholz and A. W. Kleij, *Chem. Eur. J.*, 2009, **15**, 5695; (*c*) A. W. Kleij, M. Kuil, D. M. Tooke, M. Lutz, A. L. Spek and J. N. H. Reek, *Chem. Eur. J.*, 2005, **11**, 4743; (*d*) C. T.

L. Ma and M. J. MacLachlan, *Angew. Chem. Int. Ed.*, 2005, **44**, 4178.

8. (*a*) G. Consiglio, S. Failla, P. Finocchiaro, I. P. Oliveri and S. Di Bella, *Inorg. Chem.*, 2012, **51**, 8409; (*b*) G. Consiglio, S. Failla, P. Finocchiaro, I. P. Oliveri and S. Di Bella, *Dalton Trans.*, 2012, **41**, 387; (*c*) S. Di Bella, I. P. Oliveri, A. Colombo, C. Dragonetti, S. Righetto and D. Roberto, *Dalton Trans.*, 2012, **41**, 7013; (*d*) G. Consiglio, S. Failla, P. Finocchiaro, I. P. Oliveri, R. Purrello and S. Di Bella, *Inorg. Chem.*, 2010, **49**, 5134; (*e*) G. Consiglio, S. Failla, I. P. Oliveri, R. Purrello and S. Di Bella, *Dalton Trans.*, 2009, 10426.

9. (*a*) I. P. Oliveri, S. Failla, A. Colombo, C. Dragonetti, S. Righetto and S. Di Bella, *Dalton Trans.*, 2014, **43**, 2168; (*b*) I. P. Oliveri, S. Failla, G. Malandrino and S. Di Bella, *New J. Chem.*, 2011, **35**, 2826; (*c*) I. P. Oliveri and S. Di Bella, *Tetrahedron*, 2011, **67**, 9446; (*d*) I. P. Oliveri and S. Di Bella, *J. Phys. Chem. A*, 2011, **115**, 14325.

10. See, for example: (*a*) Q. Meng, P. Zhou, F. Song, Y. Wang, G. Liu and H. Li, *CrystEngComm*, 2013, **15**, 2786; (*b*) M. Cano, L. Rodríguez, J. C. Lima, F. Pina, A. Dalla Cort, C. Pasquini and L. Schiaffino, *Inorg. Chem.*, 2009, **48**, 6229; (*c*) E. C. Escudero-Adán, J. Benet-Buchholz and A. W. Kleij, *Inorg. Chem.*, 2008, **47**, 4256; (*d*) M. E. Germain, T. R. Vargo, G. P. Khalifah and M. J. Knapp, *Inorg. Chem.*, 2007, **46**, 4422; (*e*) A. Dalla Cort, L. Mandolini, C. Pasquini, K. Rissanen, L. Russo and L. Schiaffino, *New J. Chem.*, 2007, **31**, 1633.

11. For a review, see for example: A. W. Kleij, *Dalton Trans.*, 2009, 4635.

12. I. P. Oliveri, S. Failla, G. Malandrino and S. Di Bella, *J. Phys. Chem. C*, 2013, **117**, 15335.

13. See, for example: (a) S. Fukuzumi, T. Honda, K. Ohkubo and T. Kojima, *Dalton Trans.*, 2009, 3880; (b) Y. Chen, W. Lu and C.-M. Che, *Organometallics*, 2013, **32**, 350; (c) E. Cariati, R. Macchi, D. Roberto, R. Ugo, S. Galli, N. Masciocchi and A. Sironi, *Chem. Mater.*, 2007, **19**, 3704.

14. See, for example: (*a*) Q. Jin, L. Zhang and M. Liu, *Chem. Eur. J.*, 2013, **19**, 9234; (*b*) S. Wu, J. Gao, T. J. Emge and M. A. Rogers, *Soft Matter*, 2013, **9**, 5942; (*c*) D. Canevet, Á. Pérez del Pino, D. B. Amabilino and M. Sallé, *J. Mater. Chem.*, 2011, **21**, 1428; (*d*) D. S. Tsekova, J. A. Sáez, B. Escuder and J. F. Miravet, *Soft Matter*, 2009, **5**, 3727.

15. See, for example: (*a*) X. Miao, L. Xu, Z. Li and W. Deng, *J. Phys. Chem. C*, 2011, **115**, 3358; (*b*) Y. Yang and C. Wang, *Curr. Opin. Colloid Interface Sci.*, 2009, **14**, 135.

16. I. P. Oliveri, G. Maccarrone and S. Di Bella, *J. Org. Chem.*, 2011, **76**, 8879.

17. (*a*) K. Ouari, A. Ourari and J. Weiss, *J. Chem. Crystallogr.*, 2010, **40**, 831; (*b*) A. W. Kleij, M. Kuil, M. Lutz, D. M. Tooke, A. L. Spek, P. C. J. Kamer, P. W. N. M. van Leeuwen and J. N. H. Reek, *Inorg. Chim. Acta*, 2006, **359**, 1807; (*c*) J. Reglinski, S. Morris and D. E. Stevenson, *Polyhedron*, 2002, **21**, 2175; (*d*) G. A. Morris, H. Zhou, C. L. Stern and S. T. Nguyen, *Inorg. Chem.*, 2001, **40**, 3222; (*e*) A. L. Singer and D. A. Atwood, *Inorg. Chim. Acta*, 1998, **277**, 157.

18. C. Reichardt, *Solvents and Solvent Effects in Organic Chemistry*, Third Edition; Wiley-VCH: Weinheim, 2003.
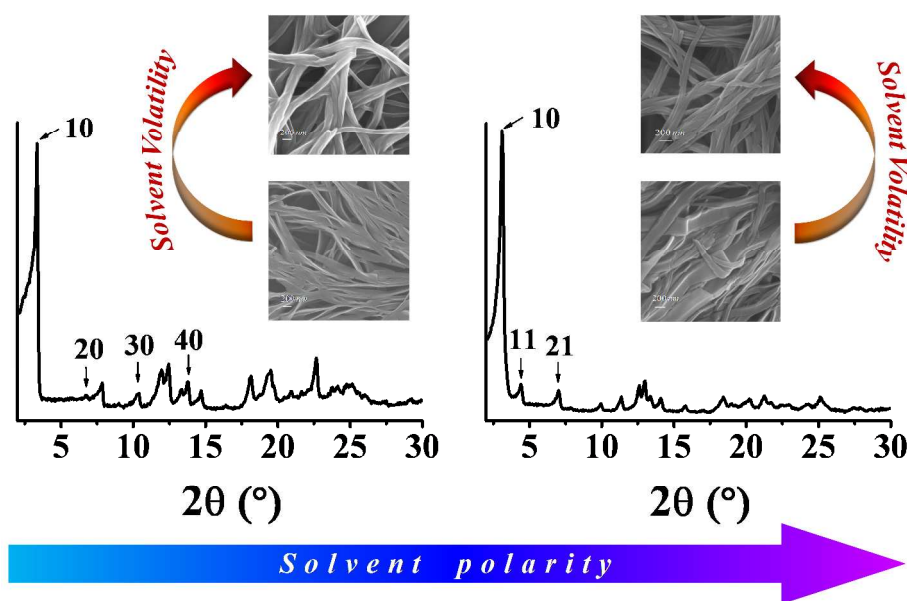
Dalton Transactions

ARTICLE TYPE

Table of Contents

Self-assembled nanostructures of amphiphilic Zinc(II) salophen complexes: role of the solvent on their structure and morphology

Ivan Pietro Oliveri, Graziella Malandrino* and Santo Di Bella*

The influence of some solvent properties, such as volatility, polarity, and Lewis basicity, on the formation of molecular self-assembled nanostructures in the solid state of an amphiphilic Zn^{II} Schiff-base complex is reported.

Dalton Transactions Accepted Manuscript